RSC Advances

Using "Underwater Superoleophobic Pattern" to Make Liquid Lens Array

Jiale Yong, Qing Yang, Feng Chen*, Guangqing Du, Chao Shan, Umar Farooq,

Jiuhong Wang, and Xun Hou

State Key Laboratory for Manufacturing System Engineering & Key Laboratory of Photonics

Technology for Information of Shaanxi Province, School of Electronics & Information

Engineering, Xi'an Jiaotong University, Xi'an, 710049, P. R. China

Corresponding author: *chenfeng@mail.xjtu.edu.cn.

Abstract

This paper reports a new strategy to realize real liquid lens array without evaporation defect based on underwater superoleophobic-oleophobic heterogeneous pattern. The flat circular region shows inherent underwater oleophobicity while the femtosecond laser ablated region performs underwater superoleophobicity. In water medium, oil droplet is restricted to the untreated circle by the energy barrier at the superoleophobic-oleophobic boundary, thereby forming the convex lens shape by surface tension. The liquid lens array benefits of the surrounding water and then overcomes the evaporation defect. The shape of the liquid lens can be simply controlled by the designed pattern and the oil volume.

1. Introduction

Lens is a common optical device and widely applied in optical communication, microscopy, light convergence/divergence, photography, laser microfabrication, and so on.[1-5] Many methods have been developed to form various lenses, including machining,[6] thermal reflow,[7] hot embossing,[8] droplet method,[9] two-photon polymerization,[10,11] and femtosecond laser wet etch.[12,13] Among those techniques, liquid lens has attracted considerable attention because of simple process, economical material, and easy adjusting for focal length.[14-16] This method relies on the surface tension of liquid droplet, such as water, to form a part-sphere shape which can be used as a convex lens. However, some defects limit the wide appellations of liquid lens. Evaporation is the most frequently mentioned disadvantage, which results in the shape of the lens being unstable because the volume decreases with time.[17] To avoid this problem, liquid polymer (for example, hydrogel and sol-gel) is used instead of water.[18,19] The liquid polymer is solidified as soon as the lens shape of the polymeric droplet forms. As a result, the lens does not meet the evaporation defect, but is at solid state. This lens is not "real" liquid lens although its formation is based on the property of liquid polymer. On the other hand, liquid lenses need to keep an enough distance from each other for preparing a lens array; otherwise they will easily mix together. The liquid lens array is usually not aligned orderly due the location of the liquid lenses is difficultly controlled. Therefore, it is still a great challenge ahead in

fabricating real uniform liquid lens array without evaporation.

Here, the glass surface is selectively ablated by femtosecond laser to form a circle array pattern, which is composed of a bare flat circle and surrounding laser-induced microstructure. The laser ablated and untreated regions respectively show underwater superoleophobicity and ordinary weak oleophobicity. The wettability difference generates an energy barrier, which can restrict oil droplet on the untreated circle. The oil droplet with part-spherical shape and the surrounding water form a converging lens.

2. Experimental

Figure 1 schematically depicts the fabrication procedure of non-evaporation liquid lens. We started with forming a circle pattern composing of bare flat untreated circle array and surrounding laser-induced region, using selective femtosecond laser ablation (Fig. 1a,b). The diameter of the circle, D, and the size of each unit, L, can be arbitrarily designed. The experimental setup and femtosecond laser ablated method were shown in our previous work.[20-22] The glass sample was fixed on a computer controlled translation stage. The laser beam (wavelength = 800 nm; pulse duration = 50 fs; repetition rate = 1 kHz) was focused on the glass surface via an objective lens (NA= 0.45, Nikon). During the line-by-line scanning process, the laser power, scanning speed, and the interval of scanning lines were set at 20 mW, 2 mm/s, and 2 μm, respectively. Turning on and off the femtosecond laser beam was controlled by a mechanical shutter. After the pattern being fabricated and cleaned, the

as-prepared sample was immersed into water. The water was treated in advance to meet the limit of solubility of oil (chloroform) although chloroform is very difficult to dissolve in water (chloroform : water = 1mL : 200mL). Then, a small oil droplet hanging a microsyringe was lowered down by a micromechanical system and contacted the untreated flat circle. Increasing volume of oil made the three-phase contract line (TPCL) go advance until reach the boundary of laser-induced and untreated domains. Because it is difficult to ensure whether the TPCL fully overlap with the edge of untreated circle, oil droplet with excess volume was placed on the flat circle in our experiment. Next, the redundant oil was sucked up until the residual amount reached designed value (Fig. 1c). During this process, the TPCL would not shrink for the contact angle hysteresis although oil volume decreased continuously.
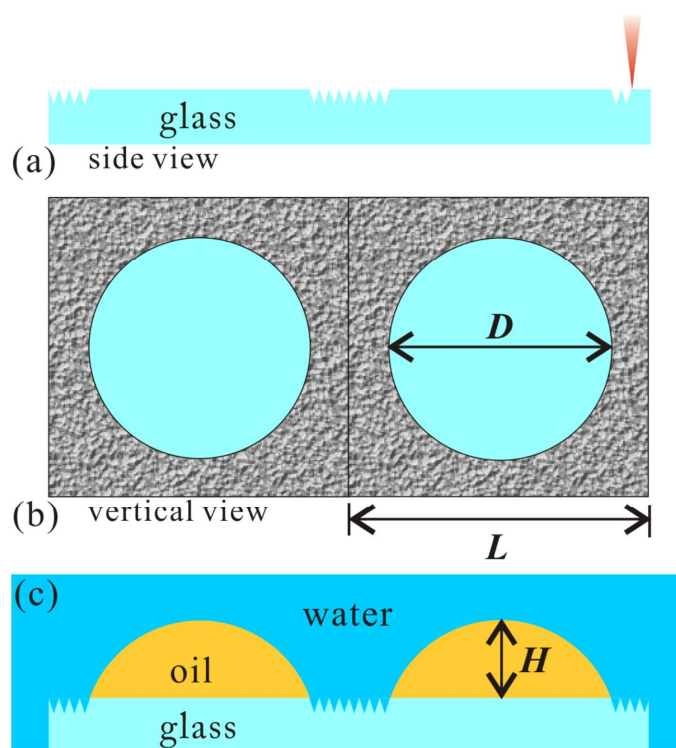
Figure 1. Schematic diagram of the formation process of liquid lens array. (a,b) Side and vertical views of

fabricating a circle array pattern composing of bare flat circle and surrounding rough microstructure by femtosecond laser selective ablation. (c) Placing the fabricated sample into water and dropping oil droplets on the bare flat circles.

3. Results and discussion

Figure 2a is the digital photo of the as-prepared surface which is composed of periodic untreated uniform circle array (6×4) and rough laser-induced region. There is a sharp boundary between untreated and laser-induced domains (Fig. 2b,c). The femtosecond laser ablated region is characterized by rough ridges with the size of several micrometers, decorating with abundant nano-particles with the diameter of just a few tens of nanometers (Fig. 2d). The surface roughness (S_a) is about 0.667 μm. The clear boundary between laser ablated and untreated regions, as well as the femtosecond laser-induced rough microstructure, is also demonstrated by its three-dimensional (3D) and cross-sectional profiles using a laser confocal scanning microscope, as shown in Figure 3. The micro/nanometer binary structures play a key role in achieving underwater superoleophobicity. Fig. 2e reveals the image of an oil droplet on the completely rough surface in a water medium. The oil droplet keeps a spherical shape, and the oil contact angle (OCA) can reach up to 160.5° ± 2°. In addition, it is very difficult to land the oil droplet on the femtosecond laser ablated surface. The oil droplet will roll off if the substrate is titled only 1°, demonstrating ultralow oil-adhesion in water (Fig. 2f). Compared with laser ablated domain, the untreated region performs inherent weak underwater oleophobicity with OCA of 121°

± 3°. Therefore, the circle array pattern is composed of underwater superoleophobic and ordinary oleophobic domains, performing a heterogeneous topography.
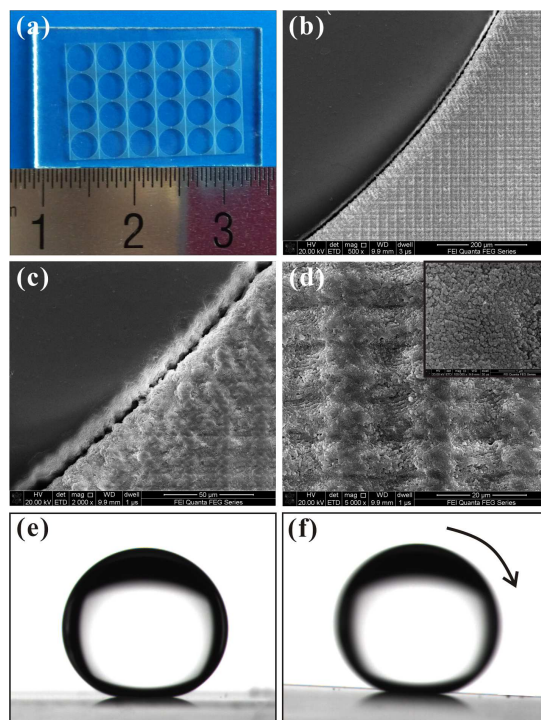
Figure 2. (a) Digital image of the as-prepared circle array pattern composing of untreated circles and rough laser induced region. (b,c) SEM image with different magnifications of the boundary between the untreated and femtosecond laser ablated regions. (d) SEM images of the femtosecond laser ablated glass surface. (e) A 8 µl oil droplet on the completely femtosecond laser ablated surface. (f) Oil droplet rolling off on the completely femtosecond laser ablated surface tiled with 1°.
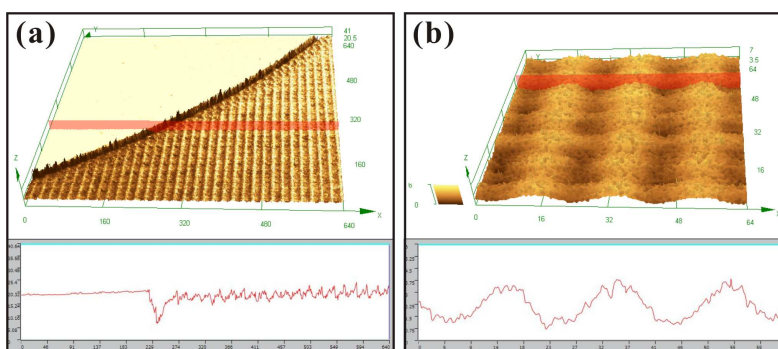
Figure 3. 3D images and cross-sectional profiles of the as-prepared pattern. (a) boundary at laser ablated and

non-ablated regions: ×400. (b) Femtosecond laser-induced microstructure: ×4000.

The glass shows an inherent hydrophilicity in the air, while its wettability can be

significantly enhanced to superhydrophilicity by femtosecond laser ablation due to

rough microstructure formation.[23] Water will immediately enter into the interspaces of

laser-induced rough microstructure as soon as the sample is immersed in water,

forming a water cushion between the oil droplet and sample. This trapped water layer

endows the oil droplet with the ability of sitting only on the top of the microstructure.

Such three-phase system (oil/water/solid) is usually described by the underwater

version of Cassie's model.[24,25] Here, the high OCA can be explained by the following

equation:

$$\cos\theta_{ow}^* = \lambda \cos\theta_{ow} + \lambda - 1 \tag{1}$$

where θ_{ow}^* and θ_{ow} are the contact angle of an oil droplet on the laser ablated

surface and bare flat glass surface in a water medium, respectively. λ is the area

fraction of the projected oil wet area. Accordingly, λ can be calculated to be 0.04 in

our experiment. This small value reveals that the underwater oil droplet only contacts

a small area of the femtosecond laser ablated rough surface. The trapped water

cushion is an ideal oil-repellent material for the repulsive interaction between

nonpolar (oil) and polar (water) molecules, endowing the femtosecond laser ablated

region with underwater superoleophobicity.[26]

In general, an energy barrier can form at the boundary between different chemical

domains or morphology with different apparent surface free energy.[27-32] Oil droplet can stick to the bare flat glass surface, which shows ordinary oleophobicity in water, even when the substrate is tilted 90° or 180°, representing a steady state. On the contrary, the underwater oil droplet on the laser ablated glass surface is at unstable state because the surface performs underwater superoleophobicity and the oil droplet can roll off easily by slight disturbance. The steady and unstable states indicate that the object is in the low and highest energy cases, respectively. Based on the Gibbs' criterion, there exists an energy barrier needing to overcome in the process of oil droplet spreading across from the flat untreated circle to the laser-induced rough region.[27,28] By gradually increasing the volume of oil droplet, oil droplet first contacts the flat untreated domain and generates strong attraction; meanwhile, the edge of the oil droplet goes advance until it reaches the boundary between untreated and laser-induced regions. Then, the energy barrier will prevent the oil droplet moving forward even with the oil volume continuing increasing. As a result, the underwater oil droplet is restricted to the untreated circle by the energy barrier at the boundary between untreated underwater ordinary oleophobic and underwater superoleophobic laser-induced regions, thereby forming a part-sphere shape for surface tension. This two-phase system, including part-sphere oil and surrounding water, can act as liquid lens.

The shape of as-prepared liquid lens can be easily controlled by the designed diameter of a circle and the oil volume. Figure 4a-c show the shapes of an underwater oil droplet on the circle pattern. It can be seen that the oil droplet is restricted on bare

flat region, keeping a partial sphere shape. With the volume increasing, the droplet

becomes bigger, while the contact area between the oil droplet and glass substrate

keeps constant. For every fabricated sample, the height (H) of a lens increases with

gradually adding oil volume (Figure 3d-f). According to our operational process of

pushing away and then sucking up oil, the range of the contact angle of the oil lens is

from the receding contact angle (~56°) of oil droplet on a flat glass surface to

advancing contact angle (~160.5°) of oil droplet on the laser-induced rough substrate.

Combining different diameter and oil volume, liquid lens performing various optical

parameters can be obtained. The controllability makes the applications of the

fabricated liquid lens more flexible and convenient. Interestingly, the underwater oil

lens is very stable, and its shape has almost no change for one week storage. This

happens because the oil droplet is immersed in water and thereby avoids evaporation,

unlike water droplets that exist in the air. The feature of non-evaporation endows the

liquid lens with long-term applications.
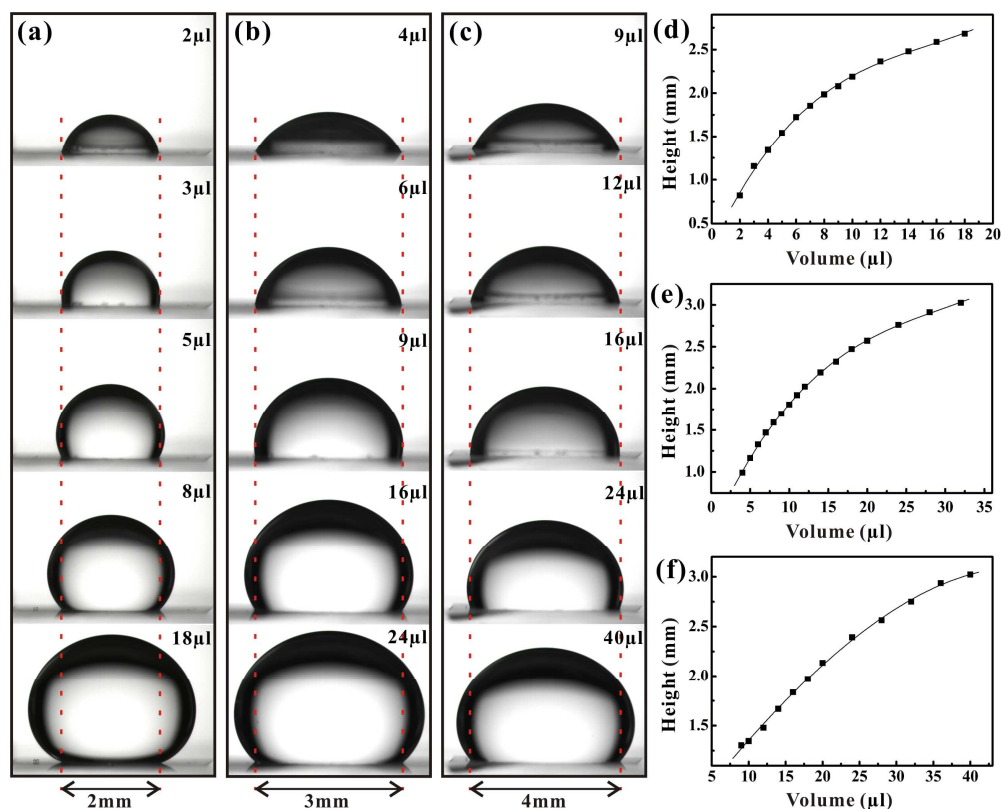
Figure 4. Controllable Shape of the as-prepared liquid lens by designed diameter of the circle and oil volume. (a-c) shapes of underwater oil droplet with different volume on the circle patterns: (a) D = 2mm, (b) D = 3mm, (c) D = 4mm. (d-f) Relationships between the height of the lens and the volume of underwater oil droplets: (d) D = 2mm, (e) D = 3mm, (f) D = 4mm.

Figure 5a,b show the digital photos of the as-prepared lens array with D = 3mm, L = 3.2 mm, and oil volume = 6μl. The H was computed to 1.33mm based on the side-shape image (Figure 4b). The oil lenses are uniformly arranged and located very close to each other. There is no need to worry that the lenses will mix together due to the good isolation effect of the femtosecond laser ablated region. Since the refractive index of water is smaller than that of chloroform, the as-prepared liquid lens composing of part-sphere oil droplet and surrounding water medium is a

converging lens. The typical optical parameters of the liquid lens array (radius of curvature, R, focal length, f, and numerical aperture, NA) can be estimated by following equations:[33,34]

$$R = \frac{(D/2)^2 + H^2}{2H}, \quad f = \frac{n_w R}{n_o - n_w}, \quad NA = \frac{D}{2f} \tag{2}$$

where n_w is the refractive index of water, and n_o is the refractive index of oil (chloroform). For example, the lenses showing in Figure 5 have D = 3 mm, H = 1.33mm, n_w = 1.33, n_o = 1.45. The R, f, and NA of those lenses are calculated as 1.51mm, 16.74mm, and 0.09, respectively. The imaging ability was tested through placing a paper with black letter "A" below the lens plane. The distance between the lens array and the object was about 20 cm. An array of inverted real image was clearly observed by a camera above the lenses, as shown in Fig. 5c. The excellent readability of the letters reflects the good imaging property and uniformity of the liquid lens array.
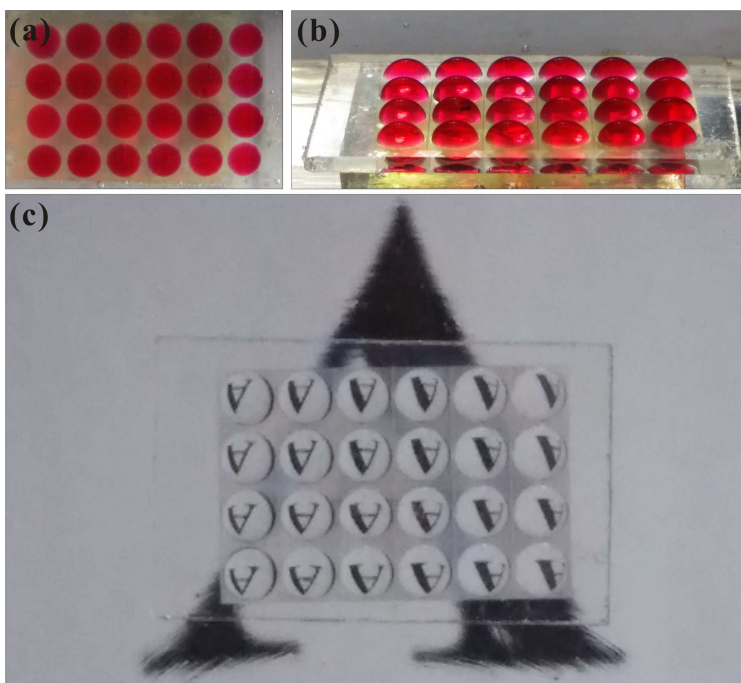
Figure 5. (a,b) Vertical and side views of the liquid lens array. For observation, the oil was dyed with Sudan □, thereby showing red color. (c) Image of an object after passing through the as-prepared liquid lens array.

4. Conclusions

In conclusion, a kind of real and uniform liquid lens array without evaporation defect was realized by an oil-water two-phase system. The glass surface is selectively ablated by femtosecond laser to form a circle array pattern, which is composed of a bare flat circle and surrounding laser-induced microstructure, showing underwater inherent oleophobicity and superoleophobicity, respectively. In water medium, oil droplet is restricted to the untreated circle by the energy barrier at the boundary of underwater superoleophobic-oleophobic heterogeneous pattern, thereby forming the convex lens shape by the surface tension. The as-prepared liquid lens array does not have the defect of evaporation because the oil droplet is in a water medium. In addition, the shape of the liquid lens can be controlled by the designed diameter of circle and the oil volume. This paper is only a proof-of-concept. In the future, the impact of the thickness of surrounding water, as well as the packaging technology, needs be further investigated. The aperture of the lens will be hopefully reduced to smaller than 1 mm as the technology becomes more accomplished.

RSC Advances Accepted Manuscript

References

(1) Y. L. Sun, W. F. Dong, R. Z. Yang, X. Meng, L. Zhang, Q. D. Chen and H. B. Sun, *Angew. Chem. Int. Ed.*, 2012, **51**, 1558.

(2) X. Li, Y. Ding, J. Shao, H. Tian and H. Liu, *Adv. Mater.*, 2012, **24**, OP165.

(3) F. Chen, Z. Deng, Q. Yang, H. Bian, G. Du, J. Si and X. Hou, *Opt. Lett.*, 2014, **39**, 606.

(4) X. H. Lee, I. Moreno and C. C. Sun, *Opt. Express*, 2013, **21**, 10612.

(5) D. X. Lu, Y. L. Zhang, D. D. Han, H. Wang, H. Xia, Q. D. Chen, H. Ding and H. B. Sun, *J. Mater. Chem. C*, 2015, **3**, 1751.

(6) A. Y. Yi and L. Li, *Opt. Lett.*, 2005, **30**, 1707.

(7) H. Yang, C. K. Chao, M. K. Wei, and C. P. Lin, *J. Micromech. Microeng.*, 2004, **14**, 1197.

(8) N. S. Ong, Y. H. Koh and Y. Q. Fu, *Microelectron. Eng.*, 2002, **60**, 365.

(9) L. Dong, A. K. Agarwal, D. J. Beebe and H. Jiang, *Nature*, 2006, **442**, 551.

(10) D. Wu, S. Z. Wu, L. G. Niu, Q. D. Chen, R. Wang, J. F. Song, H. H. Fang and H.

B. Sun, *Appl. Phys. Lett.*, 2010, **97**, 031109.

(11) D. Wu, J. N. Wang, L. G. Niu, X. L. Zhang, S. Z. Wu, Q. D. Chen, L. P. Lee and H. B. Sun, *Adv. Optical Mater.*, 2014, **2**, 751.

(12) H. Liu, F. Cheng, Q. Yang, P. Qu, S. He, X. Wang, J. Si and X. Hou, A*ppl. Phys. Lett.*, 2012, **100**, 133701.

(13) F. Chen, H. Liu, Q. Yang, X. Wang, C. Hou, H. Bian, W. Liang, J. Si and X. Hou, *Opt. Express*, 2010, **18**, 20334.

(14) C. Li and H. Jiang, *Appl. Phys. Lett.*, 2012, **100**, 231105.

(15) A. O. Ashtiani and H. Jiang, *Appl. Phys. Lett.*, 2013, **103**, 111101.

(16) Y. S. Lu, H. Tu, Y. Xu and H. Jiang, *Appl. Phys. Lett.*, 2013, **103**, 261113.

(17) Kang, C. Pang, S. M. Kim, H. S. Cho, H. S. Um, Y. W. Choi and K. Y. Suh, *Adv. Mater.*, 2012, **24**, 1709.

(18) Z. Ding and B. Ziaie, *Appl. Phys. Lett.*, 2009, **94**, 081111.

(19) X. Jin, D. Guerrero, R. Klukas and J. F. Holzman, *Appl. Phys. Lett.*, 2014, **105**, 031102.

(20) J. Yong, F. Chen, Q. Yang, G. Du, C. Shan, H. Bian, U. Farooq and X. Hou, *J. Mater. Chem. A*, DOI: 10.1039/c5ta01104c

(21) J. Yong, F. Chen, Q. Yang, D. Zhang, G. Du, J. Si, F. Yun and X. Hou, *J. Phys. Chem. C*, 2013, **117**, 24907.

(22) D. Zhang, F. Chen, Q. Yang, J. Yong, H. Bian, Y. Ou, J. Si, X. Meng and X. Hou, *ACS Appl. Mater. Interfaces*, 2012, **4**, 4905.

(23) J. Yong, F. Chen, Q. Yang, D. Zhang, U. Farooq, G. Du and X. Hou, *J. Mater.*

Chem. A, 2014, **2**, 8790.

(24) M. Liu, S. Wang, Z. Wei, Y. Song and L. Jiang, *Adv. Mater.*, 2009, **21**, 665.

(25) J. Yong, Q. Yang, F. Chen, H. Bian, G. Du, U. Farooq and X. Hou, *Adv. Mater. Interfaces*, 2015, **2**, 1400388.

(26) Q. Wen, J. Di, L. Jiang, J. Yu and R. Xu, *Chem. Sci.*, 2013, **4**, 541.

(27) J. Yong, F. Chen, Q. Yang, U. Farooq, H. Bian, G. Du and X. Hou, *Appl. Phys. Lett.*, 2014, **105**, 071608.

(28) J. Yong, Q. Yang, F. Chen, D. Zhang, U. Farooq, G. Du and X. Hou, *J. Mater. Chem. A*, 2014, **2**, 5499.

(29) L. Tie, Z. Guo and W. Li, *RSC Adv.*, 2015, **5**, 8446.

(30) W. Li and A. Amirfazli, *J. Colloid Interface Sci.*, 2005, **292**, 195.

(31) W. Li and A. Amirfazhi, *Adv. Colloid Interface Sci.*, 2007, **132**, 51.

(32) L. Tie, Z. Guo, W. Li, *J. Colloid Interface Sci.*, 2014, **436**, 19.

(33) J. Yong, F. Chen, Q. Yang, G. Du, H. Bian, D. Zhang, J. Si, F. Yun and X. Hou, *ACS Appl. Mater. Interface*, 2014, **5**, 9382.

(34) B. Hao, H. Liu, F. Chen, Q. Yang, P. Qu, G. Du, J. Si, X. Wang, and X. Hou, *Opt. Express*, 2012, **20**, 12939.